

Frequency Domain Modeling of Non-laminated C-shaped Magnetic Actuators

Lei Zhu, Carl R. Knospe, and Eric H. Maslen

Department of Mechanical and Aerospace Engineering

122 Engineers Way

University of Virginia

Charlottesville, VA 22903

lz5z@virginia.edu

crk4y@virginia.edu

ehm7s@virginia.edu

ABSTRACT

This paper employs the modeling approach previously introduced by the authors in [1] to derive an analytic model for eddy currents in a non-laminated C-shaped magnetic actuator. Due to the complexity of the original analytic model, an approximation is carried out to yield a half order simplified model. A comparison between the frequency responses of the analytic models and the results from finite element analysis demonstrates good agreement.

1. INTRODUCTION

Many magnetic actuators, for example, thrust magnetic bearings, do not have laminated construction, due to cost or strength concerns. Magnetic suspensions using non-laminated actuators usually suffer from low dynamic stiffness and low servo bandwidth. The source of these problems is the eddy currents generated in the iron when a changing current is applied to the actuator coil. An accurate analytic model for non-laminated actuators is highly desirable as it may be used during the design stage to determine the impact of actuator geometric and material properties on actuator dynamic performance.

Previously, the authors presented an analytic approach for modeling eddy currents in a non-laminated cylindrical magnetic actuator [1]. The approach is based on dividing the actuator into several elements according to the flux distribution inside the actuator, and then finding the frequency-dependent reluctance of the flux paths of each element. The frequency-dependent reluctance, which was called *effective reluctance* in [1], is an extension of the conventional concept of reluctance used in magnetic circuit theory [2]. In this paper, we will employ the same approach to derive an

analytic model for a non-laminated C-shaped actuator that is shown in Fig. 1.

Feeley [3] previously used a two-dimensional eddy current formulation for a long rectangular bar [4] to model a non-laminated C type magnetic actuator. After neglecting the summation term in the formulation, he applied an *ad hoc* approximation that resulted in a half order analytic model. However, Feeley assumes as a matter of course that the profile of flux density in a cross section of the air gap is the same as that in the associated cross section of pole iron. This is a reasonable assumption for static analysis but not for harmonic analysis because of eddy currents. An examination of the difference between our model and that provided by Feeley [3] will be presented.

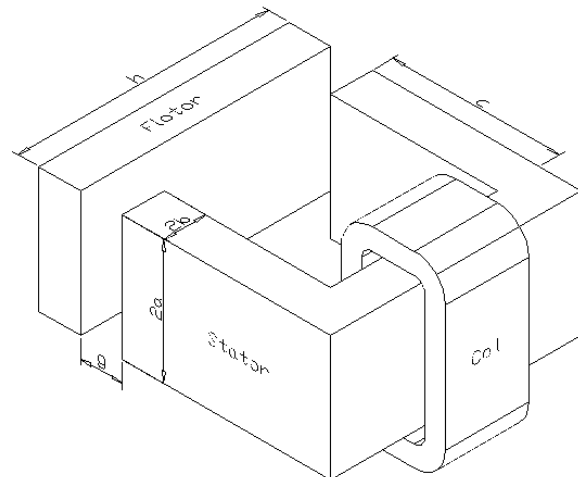


Fig. 1: C-shaped Actuator Geometry

2. ELEMENT EFFECTIVE RELUCTANCES

2.1 Actuator Geometry Division

ANSYS was used to find the flux distribution of a harmonic field inside the C-shaped actuator whose parameters are given in Table 1. Based on the flux distribution shown by ANSYS, the actuator geometry is divided into three elements, which include two air gap transition elements and an iron element, as shown in Fig. 2. Each air gap transition element contains an air gap and the associated transition iron regions in which flux changes direction. The iron element is the remains when the air gap transition elements are removed.

Table 1: C-shaped Magnetic Actuator Parameters

Parameters	Value
μ_r	1000
σ	2.5×10^6 Siemens/m
a	7.5mm
b	2.5mm
c	20mm
h	30mm
N	1200
g	0.2mm

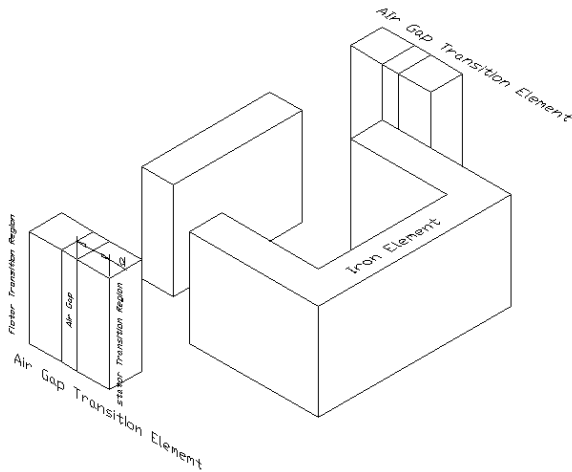


Fig. 2: Actuator Geometry Division

2.2 Effective Reluctance of Each Element

2.2.1 Effective Reluctance of an Air Gap Transition Element

Assume the flux flows from stator to flotor; the magnetic motive force (MMF) on the circumference of the stator transition region is F ; and MMF on that of the

flotor transition region is 0. Pick a point at (y, z) on the top surface of the stator transition region. The MMF at that point is $F_s(y, z)$. Under a symmetric magnetic field assumption, the MMF is $F - F_s(y, z)$ at the corresponding point on the bottom surface of the flotor transition region. Cut a small brick that contains the point out of the transition region as shown in Fig. 3.

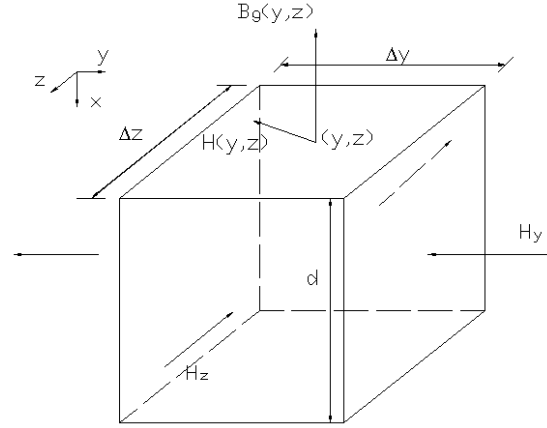


Fig. 3: A Small Brick of the Transition Region Containing (y, z) Point

Assume as usual the air gap flux is perpendicular to the transition region surfaces. Then, based on the conservation of flux, the flux entering the brick is equal to that leaving it

$$\begin{aligned}
 & \frac{F_s(y, z) - [F - F_s(y, z)]}{g} \mu_0 \Delta y \Delta z \\
 &= \left[\int_0^d H_y^s \left(y + \frac{\Delta y}{2}, z \right) \mu_r \mu_0 e^{-\alpha x} \Delta z dx \right. \\
 & \quad \left. - \int_0^d H_y^s \left(y - \frac{\Delta y}{2}, z \right) \mu_r \mu_0 e^{-\alpha x} \Delta z dx \right] \quad (1) \\
 & \quad + \left[\int_0^d H_z^s \left(y, z + \frac{\Delta z}{2} \right) \mu_r \mu_0 e^{-\alpha x} \Delta y dx \right. \\
 & \quad \left. - \int_0^d H_z^s \left(y, z - \frac{\Delta z}{2} \right) \mu_r \mu_0 e^{-\alpha x} \Delta y dx \right]
 \end{aligned}$$

where $\alpha = \sqrt{s\sigma\mu_r\mu_0}$. Equation (1) yields a partial differential equation

$$\frac{\partial^2 F_s(y, z)}{\partial y^2} + \frac{\partial^2 F_s(y, z)}{\partial z^2} = \alpha_1^2 \left[F_s(y, z) - \frac{F}{2} \right] \quad (2)$$

where $\alpha_1^2 = \frac{2\alpha}{g\mu_r}$. Using the solution of (2), we find the air gap flux,

$$\phi_g = \frac{\mu_0 AF}{g} \frac{1}{M(\alpha_1)} \quad (3)$$

where $A = 4ab$ is the cross section area, and function M is given by

$$M(v) = \left(\frac{\tanh(vb)}{vb} + \sum_{n=1}^{\infty} \frac{8}{(2n-1)^2 \pi^2} \frac{v^2 \tanh \left(a \sqrt{v^2 + \frac{(2n-1)^2 \pi^2}{4b^2}} \right)}{a \left(v^2 + \frac{(2n-1)^2 \pi^2}{4b^2} \right)^{3/2}} \right)^{-1}$$

According to the definition in [1], equation (3) yields the effective reluctance of an air gap transition element,

$$R_g = R_g^0 \cdot M(\alpha_1) \quad (4)$$

where

$$R_g^0 = \lim_{s \rightarrow 0} R_g = \frac{g}{\mu_0 A}$$

2.2.2 Effective Reluctance of the Iron Element

From [4], we know that the flux density on the cross section of the iron element is

$$B(y, z) = H_s \mu_r \mu_0 \left[\frac{\cosh(\alpha z)}{\cosh(\alpha b)} + \sum_{n=1}^{\infty} \frac{4\alpha^2}{(2n-1)\pi} \frac{\sin \frac{(2n-1)\pi}{2}}{\left(\alpha^2 + \frac{(2n-1)^2 \pi^2}{4b^2} \right) \cosh \left(\sqrt{\alpha^2 + \frac{(2n-1)^2 \pi^2}{4b^2}} a \right)} \cos \left(\frac{(2n-1)\pi}{2b} z \right) \cosh \left(\sqrt{\alpha^2 + \frac{(2n-1)^2 \pi^2}{4b^2}} y \right) \right] \quad (5)$$

From (5), we found the effective reluctance of the iron element,

$$R_i = R_i^0 \cdot M(\alpha) \quad (6)$$

where

$$R_i^0 = \lim_{s \rightarrow 0} R_i = \frac{l_i}{\mu_r \mu_0 A}$$

Equation (4) and (6) show that function M dictates how the reluctance of each element will change as frequency changes. We should point out that the argument of function M for the iron element is α while that for air gap transition elements is α_1 . This corresponds to the difference between the flux distribution on a cross section of the air gap and that on a cross section of the iron.

3. ACTUATOR TRANSFER FUNCTION

The total reluctance of the actuator is

$$R = 2R_g + R_i = 2R_g^0 M(\alpha_1) + R_i^0 M(\alpha) \quad (7)$$

Using Maxwell Stress Tensor [5], we can find the transfer function from current to air gap flux and to force for a C-shaped actuator

$$\frac{\phi_g(s)}{I_p(s)} = \frac{N}{R(s)} = \frac{N}{2R_g(s) + R_i(s)} \quad (8)$$

$$\frac{F_p(s)}{I_p(s)} = \frac{2\phi_b}{\mu_0 A} \frac{N}{2R_g(s) + R_i(s)} \quad (9)$$

where I_p is the perturbation current and ϕ_b is the actuator bias flux

$$\phi_b = \frac{NI_b}{2R_g^0 + R_i^0}$$

with I_b being the bias dc current

We now compare the total effective reluctance derived from Feeley's result and that shown in (7). While Feeley did not use the concept of effective reluctance, it is simple to determine this quantity from his result, so as to understand the limitations of his model.

Based on the two-dimensional magnetic field description for a long rectangular bar in [4], Feeley provided a formula for the air gap flux ϕ_g of a C-shaped actuator

$$\phi_g = \frac{NI_p \mu_r \mu_0 A}{l} \cdot \frac{1}{M(\alpha)} \quad (10)$$

and an approximation for (10)

$$\phi_g = \frac{NI_p \mu_r \mu_0 A}{l} \left[\frac{1}{1 + \sqrt{b^2 \sigma \mu_r \mu_0 s}} \right] \quad (11)$$

where $l = 2\mu_r g + l_i$ is the effective iron length. According to the definition in [1], (10) prescribes the total effective reluctance of a C-shaped actuator as

$$R_F = \frac{l}{\mu_r \mu_0 A} \cdot M(\alpha) \quad (12)$$

R_F can be written in the form of (7)

$$R_F = 2R_{Fg} + R_{Fi} = 2R_g^0 M(\alpha) + R_i^0 M(\alpha) \quad (13)$$

A comparison between (7) and (13) shows that in Feeley's model, the argument of function M is α for both the effective reluctance of the air gap and that of the iron. This means that Feeley has effectively assumed that the profile of flux density in a cross section of the air gap is the same as that in the associated cross section of pole iron. While this is a reasonable assumption for static analysis, it is not in the harmonic case because of eddy currents. In contrast, our model considers the variation in the flux distribution from the air gap to in the iron. In our result, the arguments for function M are α_1 and α for the air gap and the iron respectively.

4. SIMPLIFIED MODEL

Due to the complex form of R_i and R_g , a direct simplification of (8) and (9) is quite difficult to carry out. We will first approximate the effective reluctance of each element and then combine these approximations to yield simple approximations of (8) and (9).

4.1 Approximation of R_i

Numerical analysis show that when s is large

$$M(\alpha) \approx \frac{ab}{(a+b)} \cdot \alpha \quad (14)$$

and when s is very small

$$M(\alpha) \approx 1 \quad (15)$$

So an *ad-hoc* approximation \tilde{R}_i for R_i is

$$\begin{aligned} \tilde{R}_i &= R_i^0 \left(1 + \frac{ab}{a+b} \alpha\right) \\ &= R_i^0 + \frac{l_i}{4(a+b)} \sqrt{\frac{\sigma}{\mu_r \mu_0}} \sqrt{s} \end{aligned} \quad (16)$$

4.2 Approximation for R_g

Numerical analysis shows that a good approximation to $M(\alpha_1)$ is

$$\begin{aligned} &\tilde{M}(\alpha_1) \\ &= \frac{1}{\frac{\tanh(\alpha_1 b)}{\alpha_1 b} + \frac{\alpha_1^2}{\alpha_1^2 + \frac{\pi^2}{4b^2}} \frac{\tanh(a \cdot \sqrt{\alpha_1^2 + \frac{\pi^2}{4b^2}})}{a \cdot \sqrt{\alpha_1^2 + \frac{\pi^2}{4b^2}}} } \end{aligned} \quad (17)$$

Then

$$R_g \approx R_g^0 \tilde{M}(\alpha_1) \quad (18)$$

We may simplify this further by a second order Taylor series expansion of $\tilde{M}(\alpha_1)$. Since

$$\left. \frac{d\tilde{M}(\alpha_1)}{d\alpha_1} \right|_{\alpha_1=0} = 0 \quad (19a)$$

$$\begin{aligned} &\left. \frac{d^2 \tilde{M}(\alpha_1)}{d\alpha_1^2} \right|_{\alpha_1=0} \\ &= \frac{2}{3} \frac{1}{a \left(\frac{\pi}{2b}\right)^3} \left(a \cdot \left(\frac{\pi}{2b}\right)^3 b^2 - 3 \tanh\left(a \frac{\pi}{2b}\right) \right) \end{aligned} \quad (19b)$$

An approximation \tilde{R}_g for R_g is

$$\begin{aligned}\tilde{R}_g &= R_g^0 + R_g^0 \cdot \left[\frac{b^2}{3} - \frac{8b^3}{\pi^3 a} \tanh\left(\frac{\pi a}{2b}\right) \right] \cdot \alpha_1^2 \\ &= R_g^0 + \left[\frac{b}{6a} - \frac{4b^2}{\pi^3 a^2} \tanh\left(\frac{\pi a}{2b}\right) \right] \sqrt{\frac{\sigma}{\mu_r \mu_0}} \sqrt{s}\end{aligned}\quad (20)$$

Substituting approximations (16) and (20) into (8) and (9) yields a simplified model for the C-shaped actuator.

$$\frac{\phi_g(s)}{I_p(s)} = \frac{N}{2\tilde{R}_g + \tilde{R}_i} \quad (21)$$

$$\frac{F_p(s)}{I_p(s)} = \frac{2\phi_b}{\mu_0 A} \cdot \frac{N}{2\tilde{R}_g + \tilde{R}_i} \quad (22)$$

Fig.4 shows the comparison between (8) and (21) for the actuator whose parameters are given in Table 1.

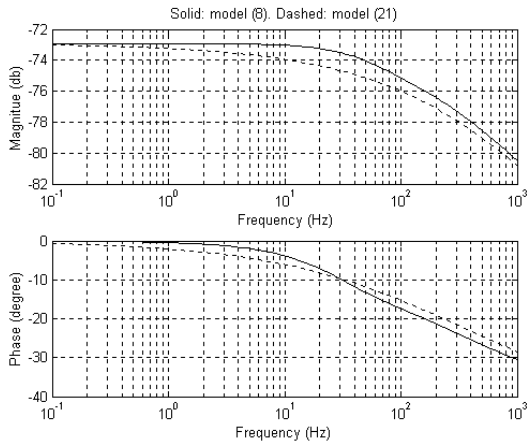


Fig. 4: Comparison Between Model (8) and Model (21)

5. COMPARISON WITH FEA

In this section, we compare the analytical models presented in Section 3 and 4 and Feeley's models with FEA results for the C-shaped actuator given in Table 1. The frequencies used in FEA are 1, 2, 5, 10, 20, 50, and 100Hz. The frequency responses of model (8), model (10) and the FEA results are shown in Fig. 5. It is clear that model (8) matches FEA results much better than Feeley's result, model (10). The author believes that the magnitude difference between model (8) and FEA will be greatly reduced if smaller element sizes were used in ANSYS (a finer mesh was not possible under our site

license). Comparison among our simplified model (21), Feeley's simplified model (21) and FEA is given in Fig. 6. Again, our approximation model matches FEA results much better than Feeley's approximation.

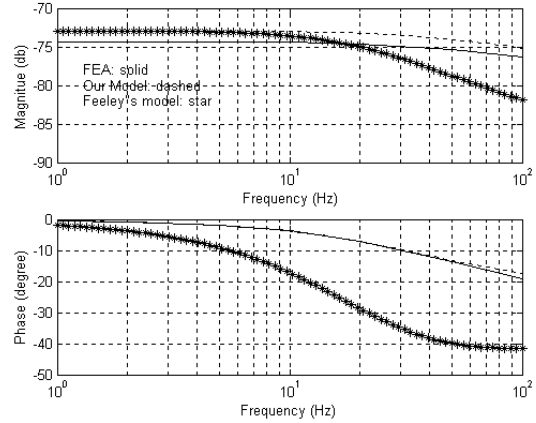


Fig. 5 Comparison among Model (8), Model (10) and FEA Results

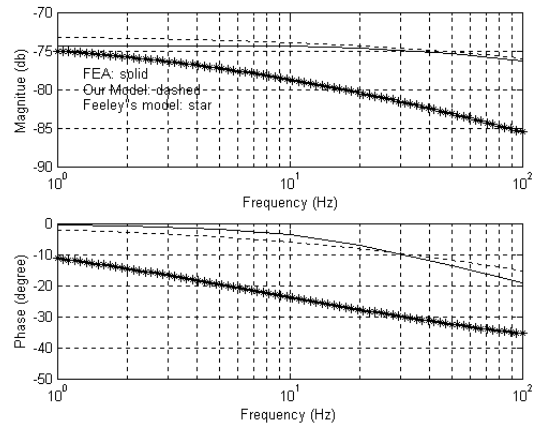


Fig. 6: Comparison among Model (11), Model (21) and FEA results

6. CONCLUSION

In this paper, we derived an analytic model for a non-laminated C-shaped magnetic actuator including eddy current effects, using the modeling approach introduced in [1]. Due to the complexity of the complete analytic model, a simplified model was developed. Comparison of the frequency responses of the two analytic models to that resulting from FEA demonstrates good accuracy. This result gives a further demonstration of the effectiveness of the modeling approach presented in [1].

Acknowledge

The authors thank the National Science Foundation for support of this research, which was funded under Grant DMII-9988877.

References

- [1] L. Zhu, C. R. Knospe, and E. H. Maslen, "Frequency Domain Modeling of Non-laminated C-shaped Magnetic Actuators", The Ninth International Symposium on Magnetic Bearings, 2004
- [2] M. A. Plonus, *Applied Electromagnetics*, McGraw-Hill, 1978
- [3] J.J. Feeley, "A simple dynamic model for eddy currents in a magnetic actuators." *IEEE Trans. Magnetics*, vol. 32, No.2, pp.453-458, Mar. 1996
- [4] R. L. Stoll, *The Analysis of Eddy Currents*. London: Oxford University Press, 1974
- [5] D. J. Griffiths. *Introduction to Electrodynamics*. New Jersey: Prentice-Hall, 1989.